Steady-state memory-phenotype conventional CD4$^+$ T cells exacerbating autoimmune neuroinflammation in bystander manner via Bhlhe40/GM-CSF axis

Je-Min Choi (✉ jeminchoi@hanyang.ac.kr)
Hanyang University https://orcid.org/0000-0002-9482-710X
Min-Zi Cho
Hanyang University
Hong-Gyun Lee
Hanyang University https://orcid.org/0000-0001-5960-5504
Jae-Won Yoon
Hanyang University
Gil-Ran Kim
Hanyang University
Ja-Hyun Koo
Hanyang University, Department of Life Science
Reshma Taneja
University of Singapore https://orcid.org/0000-0001-6214-6177
Brian Edelson
Washington University School of Medicine
You Jeong Lee
Seoul National University

Article

Keywords: Memory-phenotype CD4 T cells, CCR6, Bystander, EAE, neuroinflammation, Bhlhe40

Posted Date: November 11th, 2022

DOI: https://doi.org/10.21203/rs.3.rs-2219047/v1

Version of Record: A version of this preprint was published at Experimental & Molecular Medicine on May 1st, 2023. See the published version at https://doi.org/10.1038/s12276-023-00995-1.

Abstract

Memory-phenotype (MP) $CD4^+$ T cells are a substantial population of conventional T cells that exist in steady-state mice, and their immunologic functions in autoimmune disease have not yet been studied. In this work, we unveil a unique phenotype of MP $CD4^+$ T cells by analyzing single-cell transcriptomics and T cell receptor (TCR) repertoires. We found that steady-state MP $CD4^+$ T cells exist regardless of germ and food-antigen which are composed of heterogenous effector subpopulations. Distinct subpopulations of MP $CD4^+$ T cells are specifically activated by IL-1 family cytokines and STAT activators, revealing that the cells have TCR-independent bystander effector functions like innate lymphoid cell. Especially, $CCR6^{high}$ MP $CD4^+$ T cells are major responders to IL-1β and IL-23 without MOG_{35-55} antigen reactivity, which gives them pathogenic-Th17 characteristics and allows them to contribute to autoimmune encephalomyelitis. We identified Bhlhe40 in $CCR6^{high}$ MP $CD4^+$ T cells drives the expression of GM-CSF through IL-1β and IL-23 signaling, contributing to CNS pathology in experimental autoimmune encephalomyelitis. Collectively, our findings reveal clearly distinct effector-like heterogeneity of MP $CD4^+$ T cells in steady state and $CCR6^{high}$ MP $CD4^+$ T cells exacerbate autoimmune neuroinflammation by Bhlhe40/GM-CSF axis in bystander manner synergistically with antigen-specific T cells.

Introduction

The immunological memory of antigen-specific T cells enables faster and more potent responses upon re-exposure to a previously encountered antigen, providing long-lasting immunity [1]. Although a substantial population of memory-phenotype (MP) conventional T cells exists in steady state mice unexposed to foreign antigens, it has been reported that MP T cells are formed before birth in humans and exist in germ-free (GF) and antigen-free (AF) conditioned mice [2–6].

After undergoing homeostatic proliferation in a lymphopenic environment, naïve T cells acquire phenotypical, functional, and gene expression–like antigen-specific memory and become MP T cells [7–10]. T cell receptor (TCR) and CD28 signaling seem to be required for the conversion of naïve $CD4^+$ T cells into self-derived MP T cells in lympho-sufficient condition. These MP $CD4^+$ T cells express CD5, a marker with high affinity to self-antigen, and resist infection by mediating a Th1-like immune response without antigen stimulation [11]. A previous study confirmed that antigen-non-specific MP $CD4^+$ T cells proliferated more than Lymphocytic choriomeningitis virus (LCMV)-specific T cells in an LCMV infection model. Indeed, treatment with an anti-MHCII antibody did not inhibit the proliferation of MP $CD4^+$ T cells, suggesting that they play a bystander role against infection [12].

Unlike MP $CD4^+$ T cells, MP $CD8^+$ T cells have been well studied for their antigen-specific and bystander functions. MP $CD8^+$ T cells can rapidly produce IFN-γ upon stimulation with IL-12 and IL-18 and without cognate antigen stimulation [13,14]. In particular, MP $CD8^+$ T cells are called virtual memory. They can have specific reactions to certain antigens without previous exposure [5,15–18] and increase NKG2D and

granzyme B expression upon IL-12, IL-18, and IL-15 stimulation, producing a bystander killing role against infection [16,19,20]. In addition, MP CD8$^+$ T cells can play an antigen-specific protection role in *Listeria monocytogenes*, Herpes simplex virus (HSV), and *vaccinia* infections [5,15,18,21]. Also, MP CD8$^+$ T cells have high affinity to self-antigens, so they can break peripheral tolerance with MP CD4$^+$ T cells and develop autoimmune diabetes [22,23]. Overall, previous studies have shown the function of MP CD8$^+$ T cells in disease, but the role of MP CD4$^+$ T cells in autoimmune disease has not yet been studied.

Most previous studies have focused on the role of autoantigen-specific T cells in both humans and mice to understand autoimmune diseases and find therapeutic drugs to regulate antigen-specific T cells [24]. Interestingly, antigen-non-specific T cells, including myelin oligodendrocyte glycoprotein (MOG) tetramer–negative CD4$^+$ Th17 cells, also infiltrate the Central nervous system (CNS) in significant proportions and exacerbate experimental autoimmune encephalomyelitis (EAE) pathogenesis [25–28]. Bystander-activated T cells and Epstein-Barr virus–specific CD8$^+$ T cells are clonally expanded and correlate with disease pathogenesis in the joints of chronic inflammatory arthritis and Sjogren's syndrome patients [29–31], raising questions about the role of antigen-nonrelated T cells in autoimmune disease.

In this study, we hypothesized that MP conventional CD4$^+$ T cells could be encephalitogenic bystander cells during the development of autoimmune neuroinflammatory disease. First, we examined the heterogeneity of MP CD4$^+$ T cells using single cell RNA-sequencing (scRNA-seq) and TCR sequencing analyses. We found distinct subpopulations of Th1-, Th17-, Treg-, and Tfh-like cells among MP CD4$^+$ T cells. Those cells respond to IL-1 family cytokines and STAT activating cytokines, even without TCR stimulation. We further found that CCR6 ^{high} MP CD4$^+$ T cells are the major responders to IL-1β and IL-23, expressing pathogenic signature genes in a bystander manner and thereby contributing to the development of MOG antigen–specific T cell–derived EAE. In this context, we identified Bhlhe40 which regulates the production of GM-CSF in CCR6^{high} MP CD4$^+$ T cells in bystander manner, exacerbating EAE pathogenesis. Our findings indicate the pathogenic role of antigen independent MP CD4$^+$ T cells along with antigen-specific T cells during autoimmune neuroinflammatory disease.

Materials And Methods

Mice

C57BL/6J mice were purchased from DBL (Chungcheongbuk-do, Korea), and Rag$^{-/-}$, GM-CSF$^{-/-}$ and 2D2 TCR-transgenic mice were purchased from Jackson Laboratory (Bar Harbor, ME, USA). CD45.1$^+$, Foxp3-GFP mice were provided by Jeehee Youn (Hanyang University). GF and AF mice were purchased from the animal facility of POSTECH Biotech Center (Pohang, Korea). Bhlhe40$^{-/-}$ and Bhlhe40^{GFP} mice were provided by Brian T. Edelson (Washington University). Il1r1$^{-/-}$ mice were provided by Heung-Kyu Lee (KAIST University). The mice were housed and bred in a specific pathogen–free animal facility at Hanyang University under controlled conditions with a constant temperature (21 ± 1°C) and humidity (50

± 5%) and a 12 h light/dark cycle with regular chow and autoclaved water. All mouse experimental procedures used in this study were approved by the Institutional Animal Care and Use Committee of Hanyang University (2020-0018A,2021-005A, 2021-0158A).

MP $CD4^+$ T cell isolation and in vitro activation

MP ($TCR\beta^+CD4^+CD1d\ tetramer^-CD25^-CD62L^{low}CD44^{high}$) $CD4^+$ T cells from the spleens of 8 to 12-week-old mice were isolated using a FACS Aria II and FACS Aria Fusion cell sorter (BD Biosciences, Franklin Lakes, NJ, USA). FACS-sorted MP $CD4^+$ T cells were stimulated with IL-1β (20 ng/mL, R&D Systems, Minneapolis, MN, USA), IL-23 (20 ng/mL, R&D Systems), IL-12 (20 ng/mL, Peprotech, Rocky Hill, NJ, USA), IL-18 (20 ng/mL, R&D Systems), IL-33 (20 ng/mL, R&D Systems), IL-25 (20 ng/mL, R&D Systems), IL-7 (10 ng/mL, Peprotech, Rocky Hill, NJ, USA), or plate-bound anti-CD3/anti-CD28 (2 μg/mL, BD Biosciences) for 5 days at 37°C in an incubator.

Active EAE and adoptive transfer EAE

In active EAE model, FACS-sorted MP $CD4^+$ T cells ($\gamma\delta TCR^-NK1.1^-V_\beta11^-TCR\beta^+CD4^+CD1d\ tetramer^-Foxp3^-CD62L^{low}CD44^{high}$, 5×10^5) from Foxp3-GFP mice were adoptively transferred to 5-week-old female C57BL/6 mice. After transfer, the mice were immunized with 200 μg of MOG_{35-55} peptide in complete Freund's adjuvant (Chondrex, Inc., USA). At 0 and 48 h after immunization, the mice were intraperitoneally treated with 500 ng of pertussis toxin (List Biological Laboratories, Inc., Campbell, CA, USA). The animals were scored daily for clinical disease.

In another EAE model by adoptive transfer, naive ($CD4^+V_\beta11^+CD25^-CD62L^{high}CD44^{low}$) $CD45.1^-$ T cells ($1–5 \times 10^4$) from 2D2 TCR-transgenic mice were transferred into $Rag^{-/-}$ mice with or without WT $CCR6^{high}$ or WT $CCR6^{low}$ or $Bhlhe40^{-/-}$ $CCR6^{high}$ or $GM\text{-}CSF^{-/-}$ $CCR6^{high}$ or $GM\text{-}CSF^{-/-}$ $CCR6^{low}$ or $Il1r1^{-/-}$ $CCR6^{high}$ or $Il1r1^{-/-}$ $CCR6^{low}$MP $CD4^+$ T cells ($CD45.1^+\gamma\delta TCR^-NK1.1^-V_\beta11^-TCR\beta^+CD4^+CD1d\ tetramer^-CD25^-CD62L^{low}CD44^{high}$, 1.0×10^5). Before transfer, $CCR6^{high}$ or $CCR6^{low}$ MP $CD4^+$ T cells were primed *in vitro* with IL-7 (10 ng/mL) and IL-1β (20 ng/mL) for 5–7 days. After transfer, the mice were immunized with 100 μg of MOG_{35-55} peptide in complete Freund's adjuvant (Chondrex, Inc., USA). At 0 and 48 h after immunization, the mice were intraperitoneally treated with 200 ng of pertussis toxin (List Biological Laboratories, Inc., Campbell, CA, USA). The animals were scored daily for clinical disease as follows [32]: partially limp tail, 0.5; completely limp tail, 1; limp tail and waddling gait, 1.5; paralysis of one hind limb, 2; paralysis of one hind limb and partial paralysis of the other hind limb, 2.5; paralysis of both hind limbs, 3; ascending paralysis, 3.5; paralysis of trunk, 4; moribund, 4.5; dead, 5. On day 12 or 13, the mice were sacrificed and perfused with Phosphate buffered saline (PBS). To isolate lymphocytes, the spinal cord and brain were digested with 1 mg/mL of collagenase D (11 088 866 001; Sigma-Aldrich) and DNase I (10 104 159 001; Sigma-Aldrich) and incubated at 80 RPM on a shaker for 35 min. After enzyme digestion, lymphocytes were isolated by Percoll (GE Healthcare, Little Chalfont, UK) density-gradient centrifugation.

In vitro MOG reactivity assay (CFSE)

For antigen-specific proliferation, 2D2 naïve T cells ($CD4^+V_\beta11^+CD25^-CD62L^{high}CD44^{low}$) and $CCR6^{high}$ or $CCR6^{low}$ MP $CD4^+$ T cells ($\gamma\delta TCR^-NK1.1^-V_\beta11^-TCR\beta^+CD4^+CD1d$ tetramer$^-CD25^-CD62L^{low}CD44^{high}$) and $CD11c^+$ dendritic cells ($MHC\text{-}II^+CD11c^+$) (APC) from the spleens of 2D2 TCR-transgenic and C57BL/6 mice were isolated using a FACS Aria Fusion cell sorter. Before co-culture, naïve and MP $CD4^+$ T cells were stained with 1.25 µM carboxyfluorescein succinimidyl ester (CFSE) (Invitrogen, Carlsbad, CA) for 7 min at room temperature. After incubation, 10% Fetal bovine serum (FBS) was added, and the incubation was continued on ice for 3 min. 2D2 Naïve and $CCR6^{high}$ or WT $CCR6^{low}$ MP $CD4^+$ T cells (1×10^5 cells/well) were then washed with PBS and co-cultured with $CD11c^+$ dendritic cells (5×10^4) with or without 50 µg/mL of $MOG_{35\text{-}55}$ peptide for 72 h.

Flow cytometry

Cell surface staining was performed using the following monoclonal antibodies: anti-CD4 (RM4-5; eBioscience, San Diego, CA, USA, dilution 1:500), anti-CD25 (PC61.5; eBioscience, dilution 1:500), anti-CD44 (IM7; BioLegend, San Diego, CA, USA, dilution 1:500), anti-CD62L (MEL-14; BioLegend, dilution 1:500), anti-CD45 (30-F11, BioLegend, dilution 1:500), anti-CD45.1 (A20; eBioscience, dilution 1:500), anti-TCRβ (H57-597; eBioscience, dilution 1:500), anti-CCR6 (29-2L17; BD, dilution 1:100), anti-CXCR3 (CXCR3-173; BD, dilution 1:100), anti-$V_\alpha3.2$ (RR3-16; BioLegend, dilution 1:500), anti-$V_\beta11$ (RR3-15; BioLegend, dilution 1:500), and PE-conjugated CD1d tetramer (PBS57; NIH, dilution 1:1000). Biotinylated PBS57 loaded and unloaded CD1d monomers were provided by the US National Institutes of Health Tetramer Core facility. For intracellular staining, the cells were stimulated with a cell stimulation cocktail (00-4975-03; eBioscience) for 4 h at 37°C, and then surface markers were stained. After staining of the surface markers, the cells were fixed and permeabilized in Cytofix/Cytoperm (554714; BD Bioscience) or FOXP3/Transcription factor staining buffer set (00-5523-00; eBioscience) for 30 min at 4°C or RT. Intracellular staining was performed using the following monoclonal antibodies: anti-IL-17A (eBio17B7; eBioscience, dilution 1:200), anti-IFN-γ (XMG1.2; eBioscience, dilution 1:400), anti-GM-CSF (MP1-22E9; BD Biosciences, dilution 1:200), anti-Ki67 (SolA15; eBioscience, dilution 1:500), anti-IL-4 (11B11; BioLegend, dilution 1:200), IL-13 (eBio13A; eBioscience, dilution 1:200), anti-TNF-α (MP6-XT22; BioLegend, dilution 1:500), anti-IL-5 (TRFK5; BioLegend, dilution 1:200), anti-IL-1R1 (35F5; BD Biosciences, dilution 1:100), anti-RORγt (Q31-378; BD Biosciences, dilution 1:100), anti-T-bet (4B10; BioLegend, dilution 1:50), anti-GATA3 (L50-823; BD Bioscience, dilution 3 µl per well) and IgG1 (R2-34; BD Biosciences). Stained cells were analyzed by flow cytometry (FACS Canto II, BD Bioscience), and data were analyzed using FlowJo software version 10.8.0 (Tree Star, Ashland, OR, USA).

Cytokine (ELISA)

Samples were measured using IL-17A ELISA (432501; BioLegend), IL-13 ELISA (88-7137-88; Thermo Fisher), IL-4 ELISA (431104; BioLegend), IL-5 ELISA (431204; BioLegend), IFN-γ ELISA (430801; BioLegend), TNF-α ELISA (430904; BioLegend), and GM-CSF ELISA (432201; BioLegend) kits according to the manufacturers' instructions. Briefly, microwell plates (Corning Costar; 9018) were coated with capture

antibodies overnight at 4°C and blocked with ELISA diluent 1X for 1 h at room temperature. Samples and two-fold serial diluted standards were incubated at room temperature for 2 h, and then detection antibodies and streptavidin-HRP were added. Then, 1X TMB solution and a stop solution (2 N H_2SO_4) was loaded. The optical density was analyzed at 450 nm. Between all procedures, plates were washed at least 3 times with wash buffer (1X PBS, 0.05% Tween-20).

Statistical analysis

All data were analyzed in non-parametric analyses using the Mann-Whitney test or two-way ANOVA of variance in Prism version 8.0 (GraphPad Software, San Diego, CA). Data are presented as the mean ± S.D. or mean ± S.E.M. For all data, significance was defined as $p \leq 0.05$. Sample size and statistical information is provided in each figure legend.

Results

Single-cell RNA-sequencing identifies clearly distinct effector-like subpopulations in steady-state MP conventional CD4$^+$ T cells.

Steady-state, unprimed specific-pathogen-free (SPF)-housed mice have a significant proportion of MP CD4$^+$ T cells (TCRβ$^+$CD1d tetramer$^-$CD8$^-$CD4$^+$CD25-CD44^{high}CD62L^{low}) in their spleen, thymus, inguinal lymph nodes (iLNs), mesenteric lymph nodes (mLNs), Peyer's patches (PPs), and lung tissues (Fig. 1a and Fig. S1a, Supporting information). The proportion and number of CD4$^+$ T cells increased with age in all tissues (Fig. S1, Supporting information). To identify and focus on the characteristics of MP CD4$^+$ T cells, we used fluorescence-activated cell sorting (FACS) to sort MP CD4$^+$ T cells from the spleens of 10-week-old C57BL/6 mice and performed scRNA-seq with paired V(D)J sequencing of the T cell receptor (Fig. S2a-d, Supporting information). Also, we generated a pipeline to filter out PLZF and TCR V_α14-J_α18 (TRAV11-TRAJ18) expressing cells, a well-known key transcription factor for the development of NKT and MAIT cells [33–35]. An unbiased clustering analysis revealed clearly distinct effector T cell–like subpopulations (Fig. 1b) and differentially expressed genes (DEGs) defining each cluster (Fig. 1c and d). A Gene Ontology (GO)/Kyoto Encyclopedia of Genes and Genomes (KEGG) analysis of each cluster indicated that clusters 3 and 5 were Th1- and Th17-like populations, respectively, with significance in "chemokine-mediated signaling pathway" and "cellular response to interleukin-1" (Fig. S3, Supporting information). In addition, lineage-specific transcription factors and chemokine receptors were localized in each cluster (Fig. 1e and Fig. S4, Supporting information), suggesting that MP CD4$^+$ T cells are composed of Th1-, Th17-, Tfh-, and Treg-like subpopulations. To examine whether the subpopulations of steady-state MP CD4$^+$ T cells depended on germ or food antigens, we analyzed the proportion of CD44^{high}CD62L^{low} MP CD4$^+$ T cells in the tissues of SPF-, GF-, and AF-housed mice using flow cytometry. The proportions of total MP CD4$^+$ T cells were almost identical in the spleen and other tissues except the mLN and PP (Fig. 1f, Fig. S5a and S5b, Supporting information), indicating that the generation of splenic MP CD4$^+$ T cells is not affected by the microbiome or food antigen stimulation. Our scRNA-seq analysis

further confirmed that the SPF- and GF-housed mice had identical proportions of distinct effector-like subpopulations of splenic MP $CD4^+$ T cells (Fig. 1g and h), but the proportion of Th17-like MP cells in the mLNs of GF-housed mice was much lower than that in the mLNs of SPF-housed mice (Fig. 1i and j). In support, the proportion of $CCR6^{high}$ or $ROR\gamma t^+$ MP $CD4^+$ T cells in the mLNs of GF-housed mice was lower than that in SPF-housed mice, suggesting that the generation of gut MP $CD4^+$ T cells is specifically dependent on germs (Fig. S6, Supporting information). The TCR clonal diversity of MP $CD4^+$ T cells in GF-housed mice, especially the Th17-like population in the mLNs, was reduced compared with SPF-housed mice, though comparable diversity was observed in the spleen (Fig. 1k and l). There seemed no significant clonal expansion observed in MP subpopulations. Together, these data indicate that steady-state splenic MP $CD4^+$ T cells contain heterogeneous subpopulations of Th1-, Th17-, Tfh-, and Treg-like cells that express effector molecules and exist independently of the gut microbiome and food antigens.

Differential innate-like effector functions of MP $CD4^+$ T cells after exposure to IL-1 family and STAT activating cytokines.

To determine the effector functions of MP $CD4^+$ T cells to respond to various cytokines, we performed scRNA-seq of MP $CD4^+$ T cells cultured in conditioned medium with IL-12/IL-18, IL-25/IL-33, and IL-1β/IL-23 cytokines (Fig. 2a and Fig. S2e, Supporting information). Additionally, IL-7 was added to the culture medium for T-cell survival and maintenance [36]. The merged Uniform Manifold Approximation and Projection (UMAP) plot shows phenotypic characteristics of Th1-, Th2-, Th17-, and Treg-like subpopulations (Fig. 2b and c), which express lineage specific genes (Fig. 2d). Each cytokine set induced distinct subpopulations localized exclusively in the plot (Fig. 2e). We further confirmed the expression of selected gene sets related to the Th1, Th2, and Th17 lineages in each bystander-activated condition, which shows that type 1, 2, and 3 cytokines can upregulate lineage-specific genes in MP $CD4^+$ T cells (Fig. 2f and g). A single-cell regulatory network inference and clustering (SCENIC) analysis in each cytokine condition revealed a significant level of common or specific transcription factor activity (Fig. 2h). In addition, an Ingenuity pathway analysis (IPA) showed the predicted transcriptional regulators in each condition and speculated that the target transcription factors included Bhlhe40, which can be a potent regulator of bystander activation in MP $CD4^+$ T cells (Fig. 2i). To evaluate the effector functions of MP $CD4^+$ T cells, we treated MP $CD4^+$ T cells with those cytokines and/or anti-CD3/anti-CD28 (Fig. 2j and k). Consistently, the MP $CD4^+$ T cells responded to IL-12/IL-18, IL-25/IL-33, and IL-1β/IL-23 cytokines without TCR stimulation, and $T\text{-}bet^+IFN\text{-}\gamma^+$, $GATA3^+IL\text{-}13^+$, and $ROR\gamma t^+IL\text{-}17^+$ cells increased compared to TCR-stimulated condition (Fig. 2j). However, TNF-α was produced only in the presence of TCR stimulation and IFN-γ in the culture supernatant from IL-12/IL-18-conditioned MP $CD4^+$ T cells, and IL-4 was also significantly detected with TCR stimulation but not in the bystander condition with IL-25/IL-33. Similarly, Granulocyte-macrophage colony-stimulating factor (GM-CSF) was secreted more efficiently with IL-1β/IL-23 and TCR stimulation than with the cytokines alone (Fig. 2k). Collectively, these results indicate that steady state MP $CD4^+$ T cells have functional heterogeneity of innate-like responses to various sets of IL-

1 family and STAT activating cytokines even in the absence of T cell receptor stimulation and suggest possible potent transcriptional regulators that control MP $CD4^+$ T cell effector functions.

Potential responder MP $CD4^+$ T cells express distinct chemokine receptors upon IL-12/IL-18 and IL-1β/IL-23 stimulation.

To determine which MP $CD4^+$ T cells are potential responders to IL-1 family and STAT activating cytokines, we analyzed the subpopulation of expanding or responding clusters and performed trajectory analyses. Control MP $CD4^+$ T cells cultured with IL-7 produced a significantly separate population of $CXCR3^{high}$ cells. In IL-18/IL-12-conditioned MP $CD4^+$ T cells the $CXCR3^{high}$ cell population was reduced, and the IFN-γ- or $IL\text{-}13^{high}$expressing Th1 and proliferating Th1 populations were greatly increased (Fig. 3a and b). Th1 signature genes, *Tbx21, Ifng, Cxcr3, Il2rb1, Il18r1*, and *CCR5* were highly expressed by IL-18/IL-12-conditioned MP $CD4^+$ T cells (Fig. 3c). GO/KEGG analysis indicated that the related gene sets in those cells had increased including “Cellular response to interferon-gamma”, “Cytokine cytokine receptor interaction”, “Alzheimer’s disease”, and “Parkinson’s disease” (Fig. 3d). The IPA returned terminologies related to cytokines and inflammation such as “JAK/STAT signaling” and “neuroinflammation signaling pathway” and related to cytotoxic response including “Granzyme B signaling” (Fig. 3e). In a pseudo-time trajectory analysis, the MP $CD4^+$ T cells formed a continuous progression that started in $CXCR3^{high}$ cells and gradually progressed toward Fate 1, which expressed *Ifng, Stat5a, Bhlhe40, Batf3, Irf4* and *Irf8* (Fig. 3f and g). Similarly, a $CCR6^{high}$ cluster was present in IL-7-conditioned MP $CD4^+$ T cells, and its Th17-like cluster was specifically increased by IL-1β and IL-23 (Fig. 3h and i). Th17 signature genes, *Rorc, Ccr6, Il17a Il1r1, Il23r*, and proliferating marker *Mki67* were expressed by those cells (Fig. 3j). GO/KEGG analysis predicted that the related gene sets in IL-1β /IL-23-cultured MP $CD4^+$ T cells had increased “Alzheimer’s disease,” “Parkinson’s disease,” and “Huntington’s disease” which are neurological diseases and increased “cytokine signaling pathway” (Fig. 3k). The IPA more clearly explained the related pathways, “STAT3 pathway,” “leukocyte extravasation signaling,” “neuroinflammation signaling pathway,” “chemokine signaling,” and “Th17 activation pathway” (Fig. 3l). In the trajectory analysis, $CCR6^{high}$ cells seemed to be the starting point, and then the cells gradually differentiated toward Fate 2 (Fig. 3m), which expresses pathogenic Th17-related genes such as *Rorc, Il17a, Csf2, Il22, Bhlhe40, Rora and Cebpb* with increased activities (Fig. 3n) and expression level (Fig. 3o) of related transcriptomes. These results collectively reveal that Th1-like and Th17-like MP $CD4^+$ T cells expressing different chemokine receptors respond specifically to IL-12/IL-18 and IL-1β/IL-23 cytokines with the effector functions.

Steady state $CCR6^{high}$ memory phenotype $CD4^+$ T cells are bystander-activated by IL-1β and IL-23 to become pathogenic Th17-like cells.

Since scRNA-seq predicted that $CCR6^{high}$ cells were the major cells responding to IL-1β and IL-23, we sorted splenic $CCR6^{high}$ and $CCR6^{low}$ MP $CD4^+$ T cells (Fig. 4a and b) and then determined their proportions in steady-state SPF- and GF-housed mice (Fig. 4c). We found that splenic $CCR6^{high}$ MP $CD4^+$

T cells were independent of the gut. CCR6^{high} MP CD4^{+} T cells expressed RORγt more highly than CCR6^{low} cells and had comparable expression of T-bet (Fig. 4d). Steady-state CCR6^{high} MP CD4^{+} T cells, but not CCR6^{low}, expressed IL-17A (Fig. 4e), suggesting that CCR6^{high} MP CD4^{+} T cells are Th17-like cells. Further stimulation by IL-1β and IL-23 induced IL-17A and GM-CSF expression (Fig. 4f and g), which confirms that CCR6^{high} MP CD4^{+} T cells produce pathogenic cytokines in the bystander manner. The amount of cytokine secreted, as determined by ELISA, consistently showed that CCR6^{high} MP CD4^{+} T cells, but not CCR6^{low}, significantly produced IL-17A, GM-CSF, and IFN-γ and that IL-1β and IL-23 had important synergy for pathogenicity (Fig. 4h). In addition, IL-1β greatly expanded RORγt expression in CCR6^{high} MP CD4^{+} T cells but not CCR6^{low} cells, whereas IL-23 somewhat inhibited the proportion of Ki67-expressing cells, suggesting that IL-1β is important for the proliferation of CCR6^{high} MP CD4^{+} T cells (Fig. 4i). To further confirm the functions of IL-1β and IL-23 in MP CD4^{+} T cells, we performed bulk-RNA seq with bystander-activated MP CD4^{+} T cells exposed to IL-1β and IL-23. In the heatmap DEG analysis, IL-1β increased the expression of proliferation-related gene such as *Mki67* and *cdk2*, whereas IL-23 alone did not have any significant effects on gene expression (Fig. 4j). IL-23 and IL-1β together significantly induced the expression of pathogenic genes such as *Bhlhe40, Il1r1, Csf2*, *Ifng, Il22* and *Il17a*. In support, Gene set enrichment analysis (GSEA) pathway enrichment plot of IL-1β vs. IL-1β and IL-23 demonstrated that the enrichment score for cell proliferation was higher with IL-1β, and the score of the pathogenic Th17 signature with IL-1β and IL-23 was higher than in the control group (Fig. 4k). Through these results, we understand that steady-state CCR6^{high} MP CD4^{+} T cells, which show Th17-like characteristics, are the major bystander-activated cells responding to IL-1β and IL-23, which potentiate the cells' pathogenic character.

CCR6^{high} MP CD4^{+} T cells exacerbate autoimmune neuroinflammation in bystander manner.

To reveal the importance of splenic MP CD4^{+} T cells during an autoimmune disease, we first induced active EAE in 5-week-old mice, who have a lower proportion of MP CD4^{+} T cells than 10-week-old mice. In this mouse model, we compared the disease severity of control mice with that of those who received an additional adoptive transfer of Treg-deleted (Foxp3^{-}) MP CD4^{+} T cells from 10-week-old Foxp3-GFP mice. EAE was rapidly induced and progressed by transferring additional MP CD4^{+} T cells from 10-week-old mice, suggesting that MP CD4^{+} T cells could be an important contributor to MOG_{35-55}-induced EAE pathogenesis (Fig. S7a, Supporting information). In support, Rag$^{-/-}$ mice that adoptively transferred MOG-TCR transgenic (2D2) naïve CD45.1^{-}V$_{\beta}$11^{+}CD4^{+} T cells with Treg-deleted MP CD4^{+} T cells (CD45.1^{+}CD4^{+}) showed a more severe phenotype of EAE than the mice that received only 2D2 T cells (Fig. S7b, Supporting information), suggesting that MP CD4^{+} T cells contribute to the pathogenesis of EAE. Based on our previous results, we hypothesized that CCR6^{high} MP CD4^{+} T cells are the major pathogenic subpopulation contributing to EAE disease progression. To test that hypothesis, we transferred CCR6^{high} and CCR6^{low} MP CD4^{+} T cells (CD45.1^{+}CD4^{+}, gating strategy and purity is shown in Fig. S8, Supporting information) and 2D2 naïve CD4^{+} T cells into Rag$^{-/-}$ mice. The additional transfer of

CCR6^{high} MP CD4^{+} T cells exacerbated EAE development compared with 2D2 transfer alone or the transfer of CCR6^{low} MP CD4^{+} T cells (Fig. 5a). Interestingly, the number of transferred MP CD4^{+} T cells that appeared in the spinal cord and brain tissue did not differ between conditions (Fig. 5b). However, CCR6^{high} MP CD4^{+} T cells produced significantly more cytokines, particularly IL-17A and GM-CSF, in the spinal cord and brain tissue than CCR6^{low} MP CD4^{+} T cells (Fig. 5c and d). Therefore, CCR6^{high} MP CD4^{+} T cells, along with antigen-specific T cells, contribute to the pathogenicity of autoimmune neuroinflammation by expressing pathogenic cytokines such as IL-17A and GM-CSF. To clarify the antigen-independent activation of CCR6^{high} MP CD4^{+} T cells in an EAE mouse model, we detected 2D2 TCR ($V_{\alpha}3.2^{+}$ and $V_{\beta}11^{+}$), which are predominantly expressed in 2D2 naïve CD4^{+} T cells. Indeed, CCR6^{high} MP CD4^{+} T cells barely expressed $V_{\alpha}3.2^{+}$ and $V_{\beta}11^{+}$ (Fig. 5e and f). In support, we confirmed that steady-state CCR6^{high} and CCR6^{low} MP CD4^{+} T cells did not respond to the MOG_{35-55} antigen (Fig. 5g). Collectively, these results suggest that CCR6^{high} MP CD4^{+} T cells infiltrate in CNS tissue and exacerbate autoimmune neuroinflammation in a bystander manner.

Innate-like effector functions of CCR6^{high} MP CD4^{+} T cells are conferred by Bhlhe40/GM-CSF axis.

Among the candidate genes involved in bystander activation of CCR6^{high} MP CD4^{+} T cells, we identified that Bhlhe40/GM-CSF axis could potentially give rise to the pathogenic function of CCR6^{high} MP CD4^{+} T cells induced by IL-1β and IL-23 without TCR stimulation (Fig. 6a). By using Bhlhe40^{GFP} mice, we found that CCR6^{high} MP CD4^{+} T cells activated by IL-1β and IL-23 showed significantly increased level of Bhlhe40 (Fig. 6b). Interestingly, Bhlhe40^{GFP} positive T cells majorly produced effector cytokines including IL-17A and GM-CSF compared to Bhlhe40^{GFP} negative T cells (Fig. 6c). In support, Bhlhe40$^{-/-}$ CCR6^{high} MP CD4^{+} T cells showed markedly reduced IL-17A and GM-CSF production compared to WT (Fig. 6d and e), suggesting that Bhlhe40 is an important transcriptional regulator for the pathogenic functions of bystander CCR6^{high} MP CD4^{+} T cells. To confirm the in vivo relevance, we transferred WT CCR6^{high} or Bhlhe40$^{-/-}$ CCR6^{high} MP CD4^{+} T cells along with 2D2 naïve CD4^{+} T cells into Rag$^{-/-}$ mice. Bhlhe40$^{-/-}$ CCR6^{high} MP CD4^{+} T cells showed abrogated functions for exacerbating EAE disease compared by WT CCR6^{high} MP CD4^{+} T cells (Fig. 6f). Interestingly, the number of Bhlhe40$^{-/-}$ CCR6^{high} MP CD4^{+} T cells expressing IL-17A and GM-CSF in the spinal cord and brain tissue was significantly reduced compared to WT CCR6^{high} MP CD4^{+} T cells (Fig. 6g and h). In addition, transfer of GM-CSF-deficient CCR6^{high} MP CD4^{+} T cells showed abrogated function of contributing EAE pathogenesis (Fig. 6i), suggesting that disease aggravation by bystander CCR6^{high} MP CD4^{+} T cells is committed by IL-1β and IL-23 via Bhlhe40/GM-CSF axis. Collectively, these results indicate that Bhlhe40 confers innate-like pathogenic functions of CCR6^{high} MP CD4^{+} T cells with GM-CSF production.

Discussion

In this study, we intensively validated the characteristics of steady state MP $CD4^+$ T cells using scRNA-seq to unveil their innate-like effector functions during autoimmune disease. We found clearly distinct effector-like subpopulations in steady-state splenic MP $CD4^+$ T cells that are independent of the microbiome and food antigens. MP $CD4^+$ T cells can be bystander-activated by the different sets of IL-1 family and STAT activating cytokines. Specific chemokine receptor–expressing cells are defined as potential responder cells to each set of cytokines, and we focused on $CCR6^{high}$ MP $CD4^+$ T cells to further validate their functions in responding to IL-1β/IL-23. We demonstrated that steady state $CCR6^{high}$ MP $CD4^+$ T cells have innate-like effector functions that exacerbate EAE disease progression in a bystander manner, along with antigen-specific T cells. We suggest Bhlhe40 as a pivotal transcriptional regulator that governs GM-CSF production in bystander-activated $CCR6^{high}$ MP $CD4^+$ T cells, exacerbating EAE development. Overall, our results reveal the innate lymphoid cell-like immunological functions of steady-state MP $CD4^+$ T cells in autoimmune disease.

Innate T cells such as natural killer T (NKT), mucosal-associated invariant T (MAIT), and γδ T cells have limited TCR gene usage compared to conventional T cells, which recognize complexes of non-peptide antigens such as glycolipids, phospho-antigens, and vitamin B metabolites, respectively [37–39]. These innate T cells are derived from the thymus, which can evoke robust cytokine production. Previously, innate lymphocytes, such as NKT17, γδT17 cell, and ILC3 subsets have been defined to commonly express IL-17 and RORγt [40–42]. Furthermore, a recent study reported a novel subset of αβ-γδ co-expressing T cells which recognize MHC-restricted peptide antigens and produce effector cytokine IL-17A, GM-CSF, and IFN-γ by IL-1β and IL-23 stimulation [43]. Also, another group said that natural Th17 cells and γδ T cells expanded after the candidiasis infection model in oral cavity[44]. In this context, we carefully eliminated the possibility of contamination of innate T cells by sorting conventional MP $CD4^+$ T cells using NKT (CD1d tetramer), γδ T, αβ-γδ T, ILC, and MAIT ($TCR\beta^+CD8^-CD4^+CD25^-CD44^{high}CD62L^{low}$) exclusion gates. We confirmed that PLZF/CD1d tetramer negative steady-state MP $CD4^+$ T cells still exists as a heterogenous population containing $CCR6^{high}ROR\gamma t^+IL\text{-}17A^+$ cells, which is majorly bystander-activated by IL-1β and IL-23. Therefore, collectively, we provide compelling evidence that conventional $CD4^+$ T cells distinguished from previously known innate T cells exist, which have an innate-like features and contribute to autoimmune neuroinflammation.

As our study revealed the heterogeneous characteristics of MP $CD4^+$ T cells by single cell transcriptomic analysis, recent studies revealed the potential heterogeneity of murine MP $CD4^+$ T cells [45–47]. $CXCR3^+$T-bet^+ Th1-like MP CD4 T cells spontaneously generated from naïve $CD4^+$ T cells in steady state showed innate-like effector functions against *T. gondii* infection [11]. These cells require DC1-derived tonic IL-12 signal for optimal differentiation of T-bet^{high} MP T cells [46]. Similarly, we confirmed $CXCR3^{high}$ MP $CD4^+$ T cells are expressing T-bet and they are major responders to IL-12 and IL-18 cytokine stimulation. $CXCR3^{high}$ MP $CD4^+$ T cells, in high correlation with CCR5 expression, can produce IFN-γ and T-bet in response to IL-12 and IL-18, suggesting a innate-like function of $CXCR3^{high}$ MP $CD4^+$ T cells.

In our previous study, we demonstrated that IL-1β and IL-23 which are derived from innate immune cells[27,48–50] can synergistically potentiate the pathogenicity of memory $CD4^+$ T cells *in vitro* [26] and that non-myelin-specific $CD4^+$ T cells can infiltrate the CNS with MOG antigen–specific T cells, which significantly contribute to EAE disease progression [25,26,51,52]. In rheumatoid arthritis patients, T cells that infiltrate the synovial fluid mainly express the $CD45RO^+$ memory marker and specifically respond to epitopes of Epstein-Barr virus and cytomegalovirus [29,30,53,54]. In type 1 diabetes, infection with rotavirus or coxsackie virus is reported to be involved in accelerated diabetes onset through Toll-like receptor (TLR) signaling without pancreatic infection [55,56], and influenza A virus is linked to diabetes in human patients [57,58]. Collectively, those studies suggest that antigen-non-related $CD4^+$ T cells can contribute to disease onset or progression with antigen-specific T cells in various autoimmune diseases. We have identified here that $CCR6^{high}$ MP $CD4^+$ T cells are the major subpopulation of MP $CD4^+$ T cells that respond to IL-1β and IL-23 by expanding and inducing pathogenic Th17 characteristics. These IL-1β and IL-23 signaling In an adoptive transfer model of EAE, $CCR6^{high}$ MP $CD4^+$ T cells transferred with MOG-specific T cells induced more severe EAE than $CCR6^{low}$ cells, with increased production of IL-17 and GM-CSF in the CNS. We further confirmed that MP $CD4^+$ T cells do not respond to MOG_{33-55} antigen, indicating the innate-like functions of $CCR6^{high}$ MP $CD4^+$ T cells in autoimmune neuroinflammation. In addition, we confirmed IL-1R1 is required for pathogenic contribution of $CCR6^{high}$ MP $CD4^+$ T cells in EAE disease (Fig. S9, Supporting information) suggesting IL-1 signal to $CCR6^{high}$ MP $CD4^+$ T cells could trigger their bystander effector functions in vivo. Further studies should be done to reveal the distinct mechanism between antigen-specific T cells and bystander-activated T cells in autoimmune disease pathogenesis.

Analyzing the single cell transcriptomics of IL-1β/IL-23 responding MP $CD4^+$ T cells, we identified that Bhlhe40 could be a potential transcriptional regulator inducing GM-CSF in $CCR6^{high}$ MP $CD4^+$ T cells. Bhlhe40 has been reported to play pivotal roles in T cells. Bhlhe40-deficient naïve $CD4^+$ T cells show limited response to TCR stimulation [59]. In addition, Bhlhe40 seem to be required for Th1 and Th17 effector cytokine production including IL-17A, GM-CSF and IFN-γ in the context of autoimmune disease, GVHD, and Toxoplasma gondii infection model [27,60–62]. Expression of Bhlhe40 correlate with mouse *Csf2* locus, which encodes GM-CSF, [61,63] and also positive correlation with GM-CSF expression was reported in human PBMC [64]. We demonstrate that steady-state $CCR6^{high}$ MP $CD4^+$ T cells are expressing RORγt and IL-1 receptor that they up-regulate Bhlhe40 in response to IL-1β and IL-23. In the absence of TCR engagement, they can produce IL-17 and GM-CSF that are importantly contribute to the pathogenesis of EAE. In support, a previous study reported the majority of Bhlhe40-expressing pathogenic T cells in active EAE are non-MOG-specific [27,61]. As $Bhlhe40^{-/-}$ $CCR6^{high}$ MP $CD4^+$ T cells showed reduced GM-CSF and $GM\text{-}CSF^{-/-}$ $CCR6^{high}$ MP $CD4^+$ T cells could not exacerbate EAE, Bhlhe40/GM-CSF axis seem to be an important mechanism of bystander-activated MP $CD4^+$ T cells during EAE. Therefore, Bhlhe40 can be a pivotal transcriptional regulator for both antigen-specific and bystander MP $CD4^+$ T cells in the context of CNS inflammation and targeting of Bhlhe40 in $CD4^+$ T cells may serve as a potential novel treatment strategy to control autoimmune diseases.

Self-antigen-specific T cells are fundamentally important in triggering autoimmune inflammation; however, antigen-non-related naturally arising steady state MP $CD4^+$ T cells are also importantly contributing to pathogenic inflammation in a bystander manner. Collectively, our studies of the role that MP $CD4^+$ T cells play in neuroinflammatory disease shed light on the bystander function of adaptive immune cells to understand disease pathogenesis and reveal a novel drug development strategy to modulate autoimmune diseases.

Declarations

Acknowledgements

We thank Dr. Dongsoo Kyeong and Dr. Younhee Shin (Insilicogen Inc.) for supporting bioinformatic analysis of the scRNA-seq data. We thank Mr. Yeon-Ho Kim and Ms. In Young Song for technical support in the FACS sorting conducted at Hanyang LINC Analytical Equipment Center (Seoul) and the NIH tetramer core facility (Emory University) for providing mouse CD1d PBS-57 (Biotinylated Monomer). We thank Prof. Jeehee Youn (Hanyang University) for kindly providing $CD45.1^+$, Foxp3-GFP mice and Prof. Kwang Soon Kim (POSTECH) for helping us purchase germ-free and antigen-free mice.

Funding

This research was supported by the Basic Science Research Program (NRF-2019R1A2C3006155) of the National Research Foundation funded by the Korean government.

Author contributions

M.-Z.C., H.-G.L., and J.-M.C. conceptualized and designed this study. M.-Z.C., H.-G.L. performed and analyzed most of the experiments including bioinformatic analysis. Y.J.L. supported conceptualization for bioinformatic analyses. J.-W.Y., G.-R.K. and J.-H.K. supported experiments. R.T. and B.T.E. provided $Bhlhe40^{-/-}$ and $Bhlhe40^{GFP}$. M.-Z.C., H.-G.L., and J.-M.C. wrote draft manuscript, and all authors reviewed the manuscript. J.-M.C. supervised the analyses and acquired funding.

Conflict of Interest

The authors declare that they have no competing interests.

Data and materials availability

The data that support the findings of this study are available from the corresponding author upon reasonable request. RNA-seq data have been deposited in the NCBI Gene Expression Omnibus.

References

1. Kaech, S. M. & Cui, W. Transcriptional control of effector and memory CD8 + T cell differentiation. Nat Rev Immunol **12**, 749–761, doi:10.1038/nri3307 (2012).
2. Szabolcs, P. *et al.* Coexistent naive phenotype and higher cycling rate of cord blood T cells as compared to adult peripheral blood. Exp Hematol **31**, 708–714, doi:10.1016/s0301-472x(03)00160-7 (2003).
3. Byrne, J. A., Stankovic, A. K. & Cooper, M. D. A novel subpopulation of primed T cells in the human fetus. J Immunol **152**, 3098–3106 (1994).
4. Dobber, R., Hertogh-Huijbregts, A., Rozing, J., Bottomly, K. & Nagelkerken, L. The involvement of the intestinal microflora in the expansion of CD4 + T cells with a naive phenotype in the periphery. Dev Immunol **2**, 141–150, doi:10.1155/1992/57057 (1992).
5. Haluszczak, C. *et al.* The antigen-specific CD8 + T cell repertoire in unimmunized mice includes memory phenotype cells bearing markers of homeostatic expansion. J Exp Med **206**, 435–448, doi:10.1084/jem.20081829 (2009).
6. Kim, K. S. *et al.* Dietary antigens limit mucosal immunity by inducing regulatory T cells in the small intestine. Science **351**, 858–863, doi:10.1126/science.aac5560 (2016).
7. Ernst, B., Lee, D. S., Chang, J. M., Sprent, J. & Surh, C. D. The peptide ligands mediating positive selection in the thymus control T cell survival and homeostatic proliferation in the periphery. Immunity **11**, 173–181, doi:10.1016/s1074-7613(00)80092-8 (1999).
8. Goldrath, A. W. & Bevan, M. J. Low-affinity ligands for the TCR drive proliferation of mature CD8 + T cells in lymphopenic hosts. Immunity **11**, 183–190, doi:10.1016/s1074-7613(00)80093-x (1999).
9. Cho, B. K., Rao, V. P., Ge, Q., Eisen, H. N. & Chen, J. Homeostasis-stimulated proliferation drives naive T cells to differentiate directly into memory T cells. J Exp Med **192**, 549–556, doi:10.1084/jem.192.4.549 (2000).
10. Goldrath, A. W., Luckey, C. J., Park, R., Benoist, C. & Mathis, D. The molecular program induced in T cells undergoing homeostatic proliferation. Proc Natl Acad Sci U S A **101**, 16885–16890, doi:10.1073/pnas.0407417101 (2004).
11. Kawabe, T. *et al.* Memory-phenotype CD4(+) T cells spontaneously generated under steady-state conditions exert innate TH1-like effector function. Sci Immunol **2**, doi:10.1126/sciimmunol.aam9304 (2017).
12. Younes, S. A. *et al.* Memory phenotype CD4 T cells undergoing rapid, nonburst-like, cytokine-driven proliferation can be distinguished from antigen-experienced memory cells. PLoS Biol **9**, e1001171, doi:10.1371/journal.pbio.1001171 (2011).
13. Jacomet, F. *et al.* Evidence for eomesodermin-expressing innate-like CD8(+) KIR/NKG2A(+) T cells in human adults and cord blood samples. Eur J Immunol **45**, 1926–1933, doi:10.1002/eji.201545539 (2015).
14. Tough, D. F., Zhang, X. & Sprent, J. An IFN-gamma-dependent pathway controls stimulation of memory phenotype CD8 + T cell turnover in vivo by IL-12, IL-18, and IFN-gamma. J Immunol **166**, 6007–6011, doi:10.4049/jimmunol.166.10.6007 (2001).

15. Sosinowski, T. *et al.* CD8alpha + dendritic cell trans presentation of IL-15 to naive CD8 + T cells produces antigen-inexperienced T cells in the periphery with memory phenotype and function. J Immunol **190**, 1936–1947, doi:10.4049/jimmunol.1203149 (2013).
16. White, J. T. *et al.* Virtual memory T cells develop and mediate bystander protective immunity in an IL-15-dependent manner. Nat Commun **7**, 11291, doi:10.1038/ncomms11291 (2016).
17. Akue, A. D., Lee, J. Y. & Jameson, S. C. Derivation and maintenance of virtual memory CD8 T cells. J Immunol **188**, 2516–2523, doi:10.4049/jimmunol.1102213 (2012).
18. Hamilton, S. E., Wolkers, M. C., Schoenberger, S. P. & Jameson, S. C. The generation of protective memory-like CD8 + T cells during homeostatic proliferation requires CD4 + T cells. Nat Immunol **7**, 475–481, doi:10.1038/ni1326 (2006).
19. Chu, T. *et al.* Bystander-activated memory CD8 T cells control early pathogen load in an innate-like, NKG2D-dependent manner. Cell Rep **3**, 701–708, doi:10.1016/j.celrep.2013.02.020 (2013).
20. Lertmemongkolchai, G., Cai, G., Hunter, C. A. & Bancroft, G. J. Bystander activation of CD8 + T cells contributes to the rapid production of IFN-gamma in response to bacterial pathogens. J Immunol **166**, 1097–1105, doi:10.4049/jimmunol.166.2.1097 (2001).
21. Lee, J. Y., Hamilton, S. E., Akue, A. D., Hogquist, K. A. & Jameson, S. C. Virtual memory CD8 T cells display unique functional properties. Proc Natl Acad Sci U S A **110**, 13498–13503, doi:10.1073/pnas.1307572110 (2013).
22. Le Saout, C., Mennechet, S., Taylor, N. & Hernandez, J. Memory-like CD8 + and CD4 + T cells cooperate to break peripheral tolerance under lymphopenic conditions. Proc Natl Acad Sci U S A **105**, 19414–19419, doi:10.1073/pnas.0807743105 (2008).
23. King, C., Ilic, A., Koelsch, K. & Sarvetnick, N. Homeostatic expansion of T cells during immune insufficiency generates autoimmunity. Cell **117**, 265–277, doi:10.1016/s0092-8674(04)00335-6 (2004).
24. Serra, P. & Santamaria, P. Antigen-specific therapeutic approaches for autoimmunity. Nat Biotechnol **37**, 238–251, doi:10.1038/s41587-019-0015-4 (2019).
25. Jones, R. E., Kay, T., Keller, T. & Bourdette, D. Nonmyelin-specific T cells accelerate development of central nervous system APC and increase susceptibility to experimental autoimmune encephalomyelitis. J Immunol **170**, 831–837, doi:10.4049/jimmunol.170.2.831 (2003).
26. Lee, H. G. *et al.* Pathogenic function of bystander-activated memory-like CD4(+) T cells in autoimmune encephalomyelitis. Nat Commun **10**, 709, doi:10.1038/s41467-019-08482-w (2019).
27. Lin, C. C. *et al.* IL-1-induced Bhlhe40 identifies pathogenic T helper cells in a model of autoimmune neuroinflammation. J Exp Med **213**, 251–271, doi:10.1084/jem.20150568 (2016).
28. Lees, J. R., Sim, J. & Russell, J. H. Encephalitogenic T-cells increase numbers of CNS T-cells regardless of antigen specificity by both increasing T-cell entry and preventing egress. J Neuroimmunol **220**, 10–16, doi:10.1016/j.jneuroim.2009.11.017 (2010).
29. Tan, L. C. *et al.* Specificity of T cells in synovial fluid: high frequencies of CD8(+) T cells that are specific for certain viral epitopes. Arthritis Res **2**, 154–164, doi:10.1186/ar80 (2000).

30. Kobayashi, M., Yasui, N., Ishimaru, N., Arakaki, R. & Hayashi, Y. Development of autoimmune arthritis with aging via bystander T cell activation in the mouse model of Sjogren's syndrome. Arthritis Rheum **50**, 3974–3984, doi:10.1002/art.20679 (2004).
31. Brennan, F. M. *et al.* Resting CD4 + effector memory T cells are precursors of bystander-activated effectors: a surrogate model of rheumatoid arthritis synovial T-cell function. Arthritis Res Ther **10**, R36, doi:10.1186/ar2390 (2008).
32. Stromnes, I. M. & Goverman, J. M. Active induction of experimental allergic encephalomyelitis. Nat Protoc **1**, 1810–1819, doi:10.1038/nprot.2006.285 (2006).
33. Kovalovsky, D. *et al.* The BTB-zinc finger transcriptional regulator PLZF controls the development of invariant natural killer T cell effector functions. Nat Immunol **9**, 1055–1064, doi:10.1038/ni.1641 (2008).
34. Koay, H. F. *et al.* A three-stage intrathymic development pathway for the mucosal-associated invariant T cell lineage. Nat Immunol **17**, 1300–1311, doi:10.1038/ni.3565 (2016).
35. Savage, A. K. *et al.* The transcription factor PLZF directs the effector program of the NKT cell lineage. Immunity **29**, 391–403, doi:10.1016/j.immuni.2008.07.011 (2008).
36. Kondrack, R. M. *et al.* Interleukin 7 regulates the survival and generation of memory CD4 cells. J Exp Med **198**, 1797–1806, doi:10.1084/jem.20030735 (2003).
37. Godfrey, D. I., Uldrich, A. P., McCluskey, J., Rossjohn, J. & Moody, D. B. The burgeoning family of unconventional T cells. Nat Immunol **16**, 1114–1123, doi:10.1038/ni.3298 (2015).
38. Pellicci, D. G., Koay, H. F. & Berzins, S. P. Thymic development of unconventional T cells: how NKT cells, MAIT cells and gammadelta T cells emerge. Nat Rev Immunol **20**, 756–770, doi:10.1038/s41577-020-0345-y (2020).
39. Lee, M. *et al.* Single-cell RNA sequencing identifies shared differentiation paths of mouse thymic innate T cells. Nat Commun **11**, 4367, doi:10.1038/s41467-020-18155-8 (2020).
40. Lee, Y. J., Holzapfel, K. L., Zhu, J., Jameson, S. C. & Hogquist, K. A. Steady-state production of IL-4 modulates immunity in mouse strains and is determined by lineage diversity of iNKT cells. Nat Immunol **14**, 1146–1154, doi:10.1038/ni.2731 (2013).
41. Walker, J. A., Barlow, J. L. & McKenzie, A. N. Innate lymphoid cells–how did we miss them? Nat Rev Immunol **13**, 75–87, doi:10.1038/nri3349 (2013).
42. Sutton, C. E. *et al.* Interleukin-1 and IL-23 induce innate IL-17 production from gammadelta T cells, amplifying Th17 responses and autoimmunity. Immunity **31**, 331–341, doi:10.1016/j.immuni.2009.08.001 (2009).
43. Edwards, S. C. *et al.* A population of proinflammatory T cells coexpresses alphabeta and gammadelta T cell receptors in mice and humans. J Exp Med **217**, doi:10.1084/jem.20190834 (2020).
44. Conti, H. R. *et al.* Oral-resident natural Th17 cells and gammadelta T cells control opportunistic Candida albicans infections. J Exp Med **211**, 2075–2084, doi:10.1084/jem.20130877 (2014).

45. ElTanbouly, M. A. *et al.* VISTA is a checkpoint regulator for naive T cell quiescence and peripheral tolerance. Science **367**, doi:10.1126/science.aay0524 (2020).
46. Kawabe, T. *et al.* Requirements for the differentiation of innate T-bet(high) memory-phenotype CD4(+) T lymphocytes under steady state. Nat Commun **11**, 3366, doi:10.1038/s41467-020-17136-1 (2020).
47. Kawabe, T. *et al.* Redefining the Foreign Antigen and Self-Driven Memory CD4(+) T-Cell Compartments via Transcriptomic, Phenotypic, and Functional Analyses. Front Immunol **13**, 870542, doi:10.3389/fimmu.2022.870542 (2022).
48. McGinley, A. M. *et al.* Interleukin-17A Serves a Priming Role in Autoimmunity by Recruiting IL-1beta-Producing Myeloid Cells that Promote Pathogenic T Cells. *Immunity* **52**, 342–356 e346, doi:10.1016/j.immuni.2020.01.002 (2020).
49. Levesque, S. A. *et al.* Myeloid cell transmigration across the CNS vasculature triggers IL-1beta-driven neuroinflammation during autoimmune encephalomyelitis in mice. J Exp Med **213**, 929–949, doi:10.1084/jem.20151437 (2016).
50. Croxford, A. L. *et al.* The Cytokine GM-CSF Drives the Inflammatory Signature of CCR2 + Monocytes and Licenses Autoimmunity. Immunity **43**, 502–514, doi:10.1016/j.immuni.2015.08.010 (2015).
51. Shim, C. H., Cho, S., Shin, Y. M. & Choi, J. M. Emerging role of bystander T cell activation in autoimmune diseases. BMB Rep **55**, 57–64 (2022).
52. Lee, H. G., Cho, M. Z. & Choi, J. M. Bystander CD4(+) T cells: crossroads between innate and adaptive immunity. Exp Mol Med **52**, 1255–1263, doi:10.1038/s12276-020-00486-7 (2020).
53. Scotet, E. *et al.* Frequent enrichment for CD8 T cells reactive against common herpes viruses in chronic inflammatory lesions: towards a reassessment of the physiopathological significance of T cell clonal expansions found in autoimmune inflammatory processes. Eur J Immunol **29**, 973–985, doi:10.1002/(SICI)1521-4141(199903)29:03<973::AID-IMMU973>3.0.CO;2-P (1999).
54. Pacheco, Y. *et al.* Bystander activation and autoimmunity. J Autoimmun **103**, 102301, doi:10.1016/j.jaut.2019.06.012 (2019).
55. Pane, J. A., Webster, N. L. & Coulson, B. S. Rotavirus activates lymphocytes from non-obese diabetic mice by triggering toll-like receptor 7 signaling and interferon production in plasmacytoid dendritic cells. PLoS Pathog **10**, e1003998, doi:10.1371/journal.ppat.1003998 (2014).
56. Horwitz, M. S. *et al.* Diabetes induced by Coxsackie virus: initiation by bystander damage and not molecular mimicry. Nat Med **4**, 781–785, doi:10.1038/nm0798-781 (1998).
57. Pane, J. A. & Coulson, B. S. Lessons from the mouse: potential contribution of bystander lymphocyte activation by viruses to human type 1 diabetes. Diabetologia **58**, 1149–1159, doi:10.1007/s00125-015-3562-3 (2015).
58. Nenna, R. *et al.* Detection of respiratory viruses in the 2009 winter season in Rome: 2009 influenza A (H1N1) complications in children and concomitant type 1 diabetes onset. Int J Immunopathol Pharmacol **24**, 651–659, doi:10.1177/039463201102400311 (2011).
59. Martinez-Llordella, M. *et al.* CD28-inducible transcription factor DEC1 is required for efficient autoreactive CD4 + T cell response. J Exp Med **210**, 1603–1619, doi:10.1084/jem.20122387 (2013).

60. Piper, C. *et al.* Pathogenic Bhlhe40 + GM-CSF + CD4 + T cells promote indirect alloantigen presentation in the GI tract during GVHD. Blood **135**, 568–581, doi:10.1182/blood.2019001696 (2020).
61. Lin, C. C. *et al.* Bhlhe40 controls cytokine production by T cells and is essential for pathogenicity in autoimmune neuroinflammation. Nat Commun **5**, 3551, doi:10.1038/ncomms4551 (2014).
62. Yu, F. *et al.* The transcription factor Bhlhe40 is a switch of inflammatory versus antiinflammatory Th1 cell fate determination. J Exp Med **215**, 1813–1821, doi:10.1084/jem.20170155 (2018).
63. Jarjour, N. N. *et al.* BHLHE40 Promotes TH2 Cell-Mediated Antihelminth Immunity and Reveals Cooperative CSF2RB Family Cytokines. J Immunol **204**, 923–932, doi:10.4049/jimmunol.1900978 (2020).
64. Emming, S. *et al.* A molecular network regulating the proinflammatory phenotype of human memory T lymphocytes. Nat Immunol **21**, 388–399, doi:10.1038/s41590-020-0622-8 (2020).

Figures

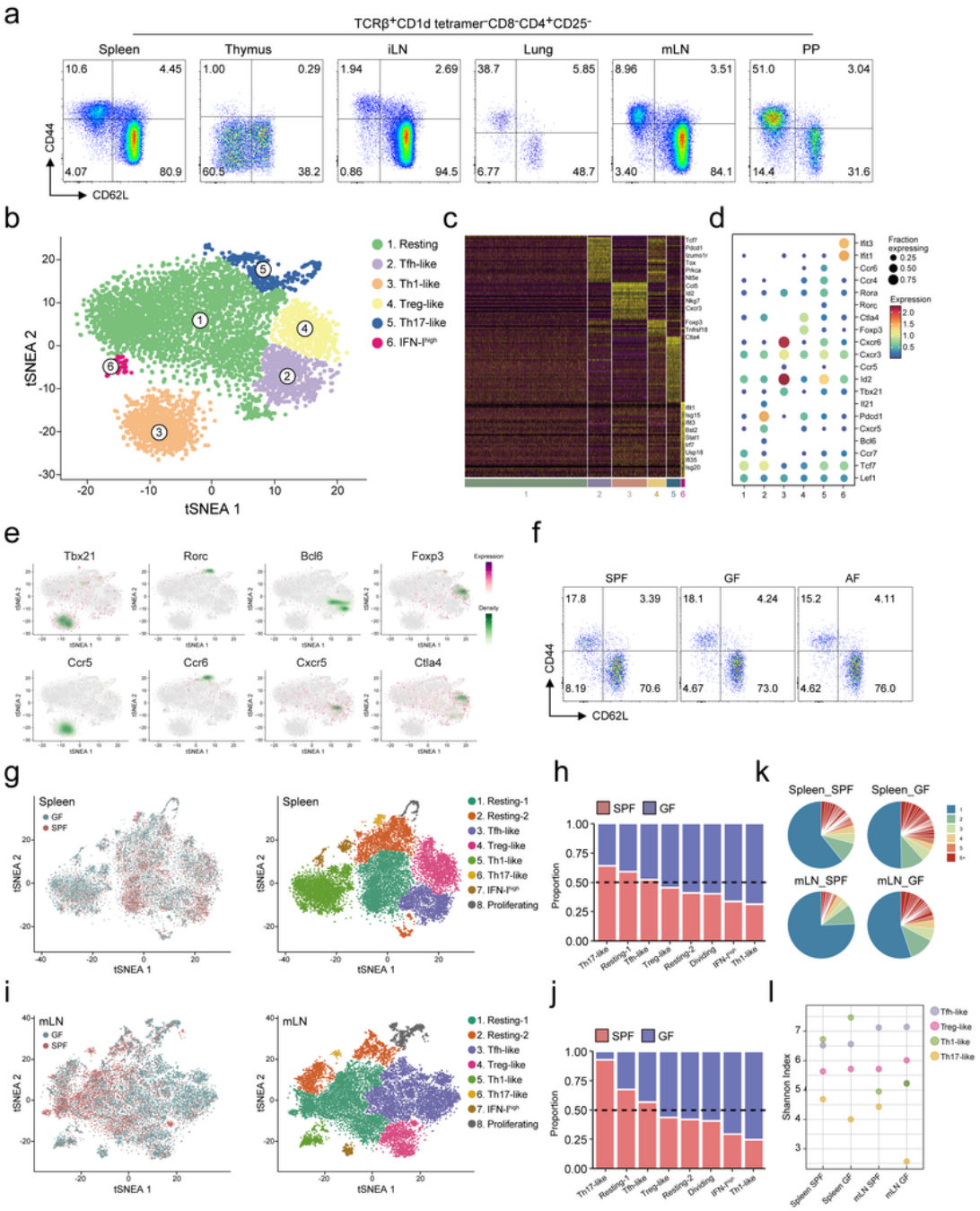

Figure 1

Single cell RNA-sequencing identifies clearly distinct effector-like subpopulations in steady-state MP CD4$^+$ T cells. (a) Representative flow cytometry plots showing the population of memory-phenotype (MP) CD4$^+$ T cells (TCRβ$^+$CD1d tetramer$^-$CD8$^-$CD4$^+$CD25$^-$CD62L^{low}CD44^{high}) in murine spleens, thymuses, inguinal lymph nodes (iLNs), lungs, mesenteric lymph nodes (mLNs), and Peyer's patches (PP). (b) tSNE plot of splenic MP CD4$^+$ T cells isolated from 10-week-old specific-pathogen-free (SPF) mice. (c)

Heatmap of differentially expressed transcripts in splenic MP $CD4^+$ T cells. (d) Expression of selected genes used to define MP $CD4^+$ T cell clusters. (e) Differential expression of transcription factors and chemokine receptors from splenic MP $CD4^+$ T cell clusters. (f) Flow cytometry plots of splenic MP $CD4^+$ T cells ($TCR\beta^+CD1d\ tetramer^-CD8^-CD4^+CD25^-CD62L^{low}CD44^{high}$) from SPF-, GF-, and AF-mice. (g) tSNE plot and (h) proportion of integrated splenic MP $CD4^+$ T cells isolated from 10-week-old SPF- and GF-mice. (i) tSNE plot and (j) proportion of integrated mLN MP $CD4^+$ T cells isolated from SPF- and GF-mice. (k) Pie chart representing the clonal size distribution of MP $CD4^+$ T cells. (l) Diversity of the TCR repertoire in MP $CD4^+$ T cell subsets from SPF- and GF-mice.

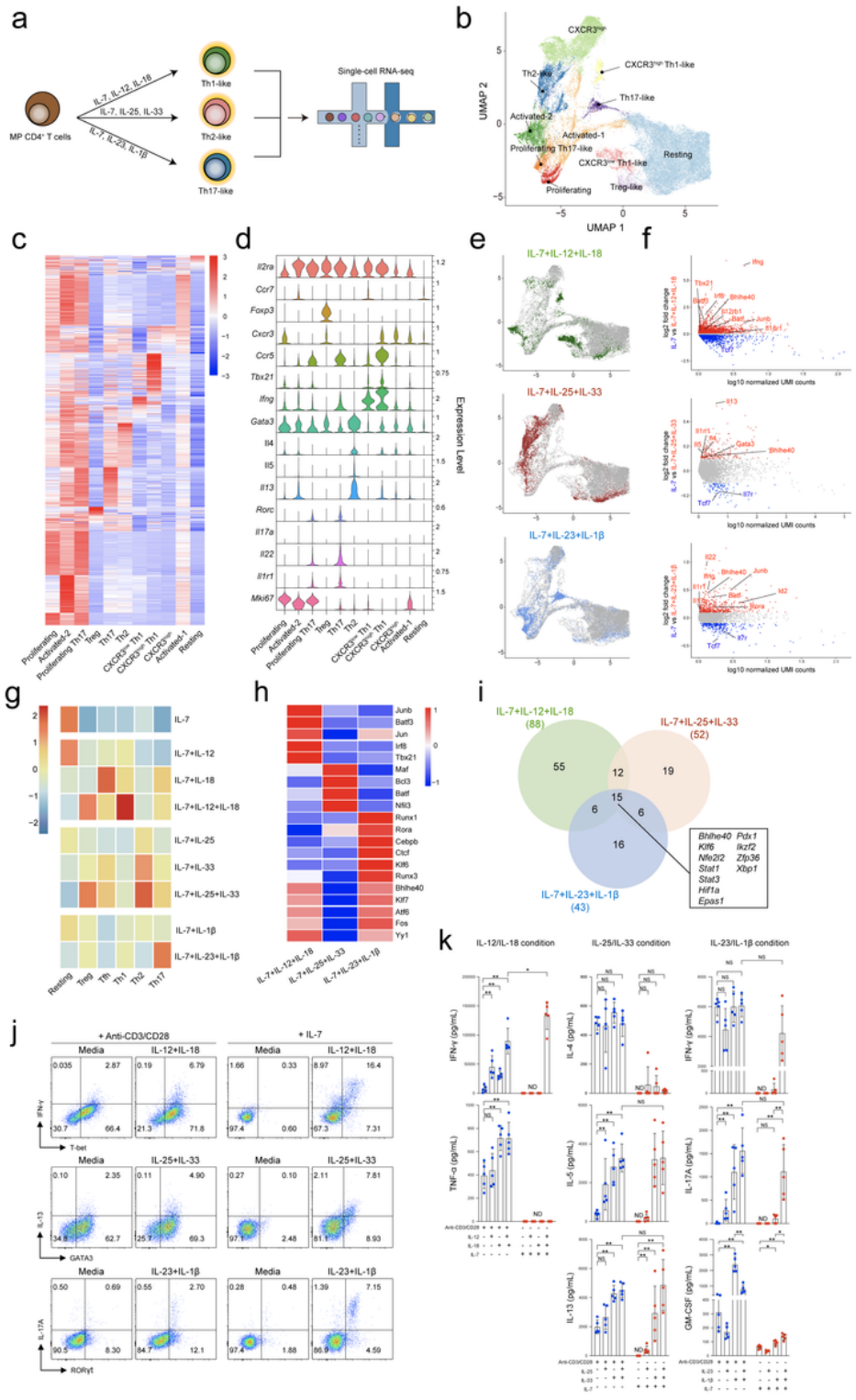

Figure 2

Differential innate-like effector functions of MP CD4$^+$ T cells after exposure to IL-1 family and STAT activating cytokines. (a) Overview of experimental design. (b) UMAP representation of MP CD4$^+$ T cells stimulated with IL-12 and/or IL-18 and IL-33 and/or IL-25 and IL-1β and/or IL-23 in the presence of IL-7. (c) Heatmap and (d) violin plots of differentially expressed transcripts in cluster. (e) Individual cytokines conditions visualized with UMAP. (f) MA plots of differentially expressed genes comparing IL-7 versus IL-

12/18 or IL-33/25 or IL-1β/23. (g) Heatmap representing gene expression of Resting-, Tfh-, Th1-, Th2-, Th17- and Treg-related gene signatures in each cytokine condition. (h) Heatmap representing transcription activity. (i) Venn diagram of transcriptional regulators predicted by the IPA. Numbers indicate the number of gene in each gate. (j) MP $CD4^+$ T cells ($TCR\beta^+CD1d$ $tetramer^-CD8^-CD4^+CD25^-CD62L^{low}CD44^{high}$) were cultured for 5 days with IL-12 and/or IL-18 and IL-33 and/or IL-25 and IL-1β and/or IL-23 in the presence of IL-7 or anti-CD3/anti-CD28. Representative flow cytometry plots showing the expression of effector lineage markers in each cytokine condition. (k) IFN-γ, TNF-α, IL-4, IL-5, IL-13, IL-17A, and GM-CSF were measured by ELISA (n=5, 5 independent experiments). Data are presented as the mean ± S.D. P values were calculated using Mann-Whitney U-test (*$p < 0.05$, **$p < 0.01$, ***$p < 0.001$).

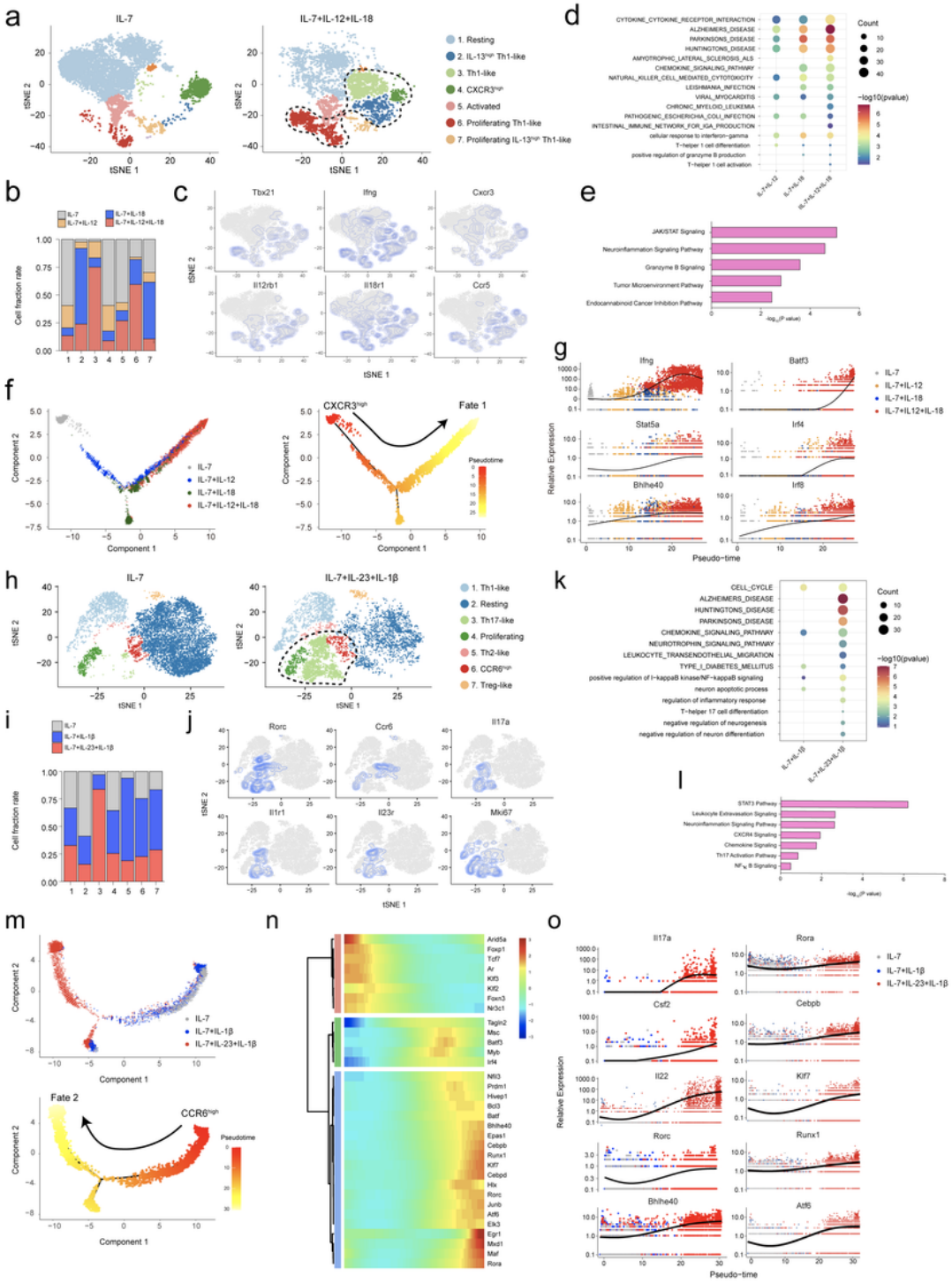

Figure 3

Potential responder MP CD4$^+$ T cells express distinct chemokine receptors upon IL-12/IL-18 and IL-1β /IL-23 stimulation. (a) tSNE plots and (b) proportion of MP CD4$^+$ T cells stimulated with IL-12 and IL-18 in the presence of IL-7 for 5 days. (c) Expression of selected Th1-related genes. (d) Selected KEGG/GO terms in cluster 2,3,4 and 6 and (e) Ingenuity pathway analysis (IPA) in cluster 3,4 and 6 of IL-12- and IL-18-responded MP CD4$^+$ T cells. (f) Pseudo-time trajectory: each cell is colored by its pseudo-time value and

(g) the expression level of the related genes. (h) tSNE plots and (i) proportion of MP CD4$^+$ T cells stimulated with IL-1β and IL-23 in the presence of IL-7 for 5 days. (j) Expression of selected Th17-related genes. (k) Selected KEGG/GO terms and (l) IPA of IL-1β- and IL-23-stimulated MP CD4$^+$ T cells (clusters 3, 4, 6). (m) Pseudo-times trajectory: each cell is colored by its pseudo-time value and (n) the transcription factor activity and (o) expression level of the related genes.

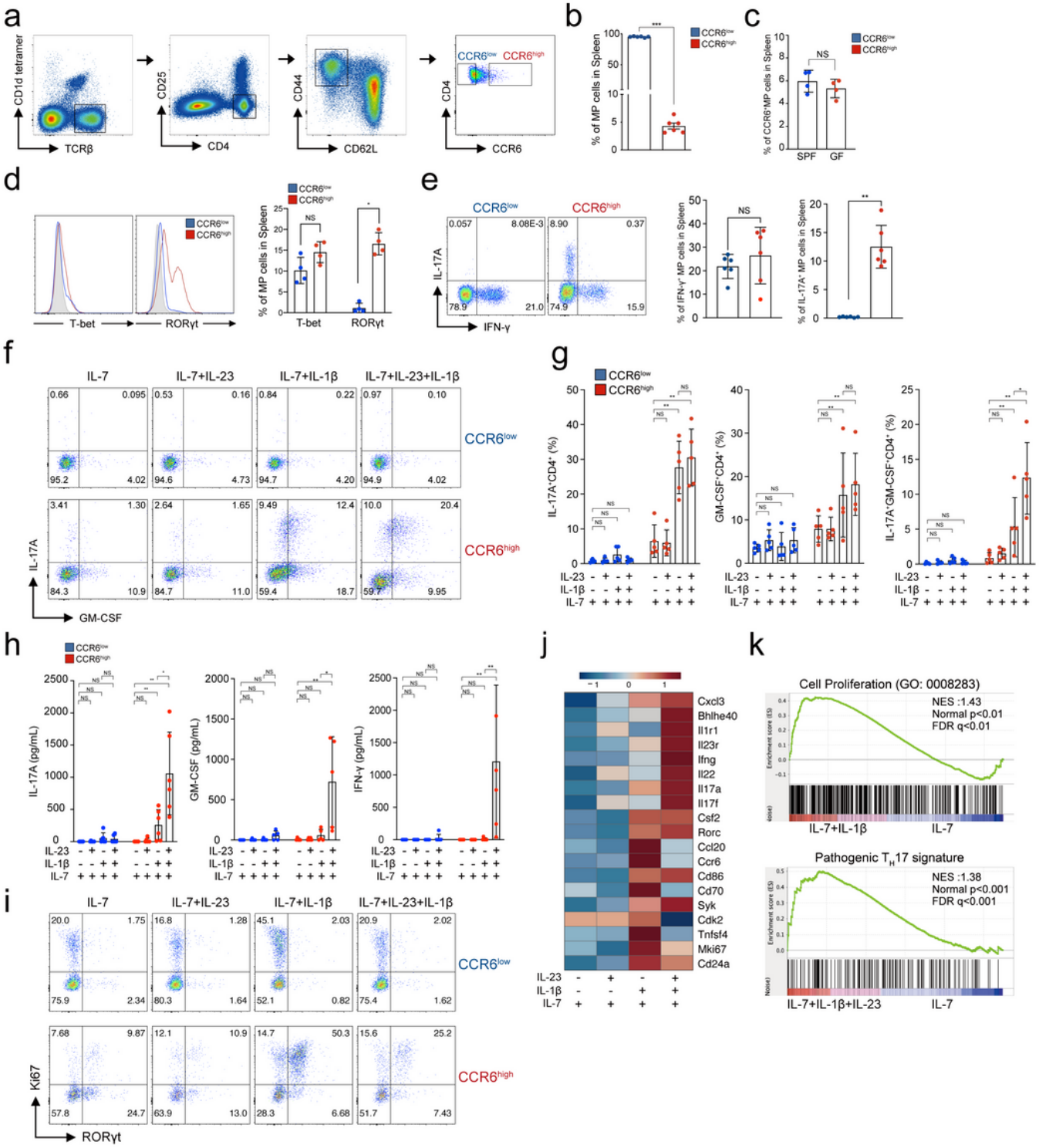

Figure 4

Steady state CCR6^{high} MP CD4^{+} T cells are bystander-activated by IL-1β and IL-23 to become pathogenic Th17-like cells. (a) Gating strategy of CCR6^{high} and CCR6^{low} MP CD4^{+} T cells from SPF mice. (b) The percentage of CCR6 expression in steady-state splenic MP CD4^{+} T cells (n=6). (c) The expression of CCR6 in SPF- vs. GF-MP CD4^{+} T cells (n=4). (d) Transcription factor expression level of T-bet and RORγt in FACS-sorted CCR6^{high} and CCR6^{low} MP CD4^{+} T cells and (e) cytokine expression and the average proportion of CCR6^{high} MP CD4^{+} T cells vs. CCR6^{low} MP CD4^{+} T cells (n = 6). CCR6^{high} and CCR6^{low} MP CD4^{+} T cells were stimulated with IL-1β and/or IL-23 in the presence of IL-7 for 5 days. (f) The representative proportion and (g) the average value showing the cytokine producing cells (n=5). (h) Concentration of IL-17A, GM-CSF, and IFN-γ were analyzed by ELISA (n = 5). (i) The proportion of RORγt^{+} and Ki67^{+} cells in CCR6^{high} and CCR6^{low} MP CD4^{+} T cells. (j) Heatmap of selected genes (k) Gene set enrichment analysis (GSEA) pathway enrichment plot related to “Cell Proliferation” and “Pathogenic T_H17 signature” by bulk RNA-seq analysis. *q*, false discovery rate; NES, normalized enrichment score. Data are presented as the mean ± S.D. All data of p values were calculated using Mann-Whitney U-test (ND, not detected; NS, not significant; *p < 0.05, **p < 0.01, ***p < 0.001).

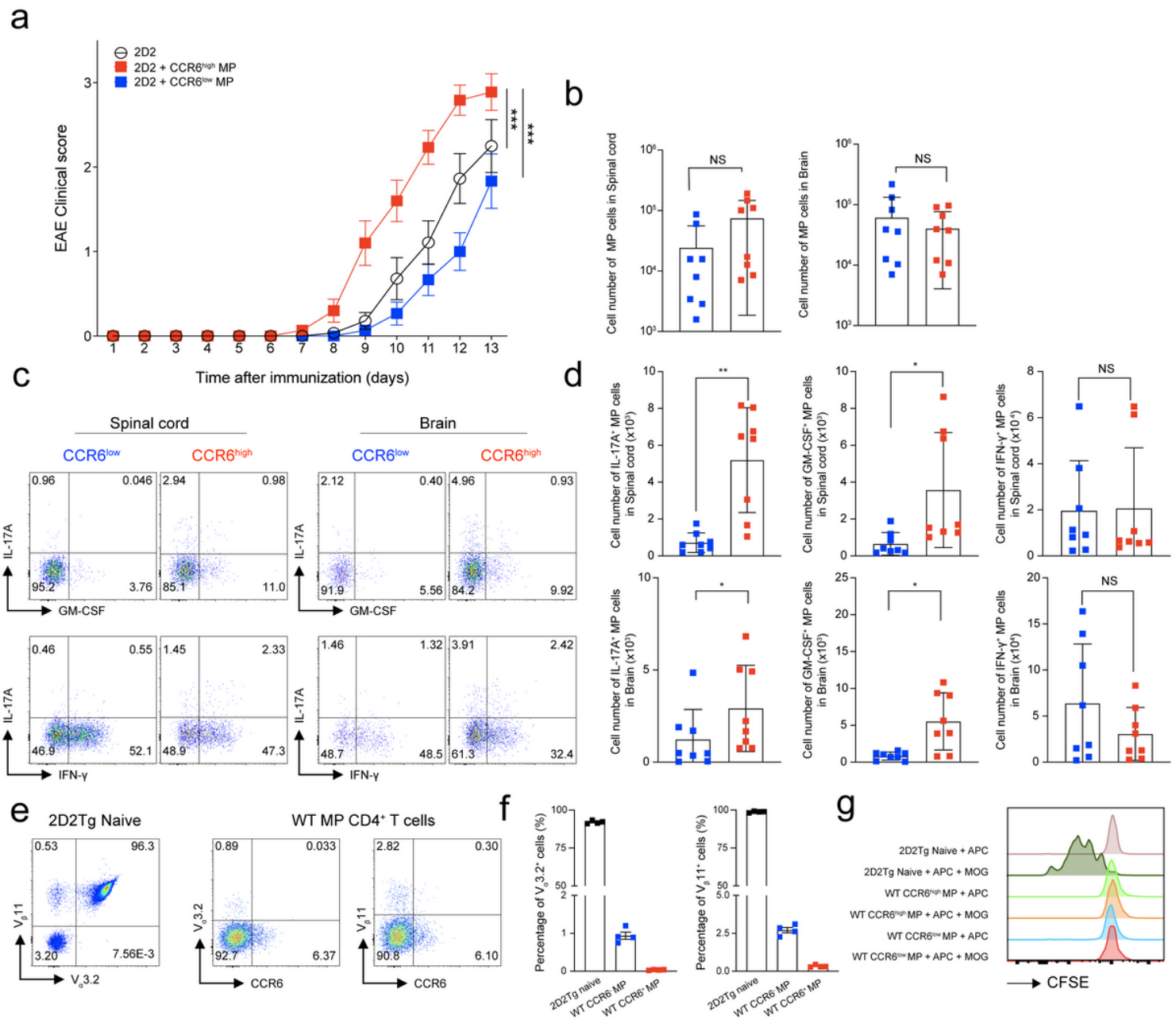

Figure 5

CCR6^{high} MP CD4^{+} T cells exacerbate autoimmune neuroinflammation in bystander manner. (a) Naïve CD4^{+} T cells (5 × 10^{4}) from 2D2 transgenic mice were adoptively transferred, with or without CCR6^{high} or CCR6^{low} MP CD4^{+} T cells (1 × 10^{5}, CD45.1^{+}γδTCR^{-}NK1.1^{-}V$_{β}$11^{-}TCRβ^{+}CD4^{+}CD1d tetramer^{-}CD25^{-} CD62L^{low}CD44^{high}), into Rag$^{-/-}$ mice who were immunized with MOG$_{35-55}$ in CFA. EAE clinical score was monitored daily (n=15). (b) Absolute cell numbers of infiltrated CD45.1^{+}MP CD4^{+} T cells in the spinal cord and brain (n=8). (c) The representative plots and (d) absolute cell number of IL-17A, GM-CSF, and IFN-γ producing cells were determined in MP CD4^{+} T cells from the spinal cords and brains on days 12–13 after immunization (n=8). (e) The representative dot plots and (f) the average value showing the

percentage of 2D2 TCR ($V_{\alpha}3.2^{+}$ and $V_{\beta}11^{+}$) in spleens from 2D2 transgenic mice and C57BL/6 wild type mice (n=4). (g) FACS-sorted 2D2 naïve $CD4^{+}$ T cells and $CCR6^{high}$ or $CCR6^{low}$ MP $CD4^{+}$ T cells were cultured with $CD11c^{+}$ dendritic cells ($MHC\text{-}II^{+}CD11c^{+}$) with or without $MOG_{35\text{-}55}$ peptide (50 µg/ml) for 3 days. CFSE levels were measured by flow cytometry. Data are presented as the mean ± S.E.M in a and the mean ± S.D in b,d,f. *P* values were calculated using two-way ANOVA or Mann-Whitney U-test (NS, not significant; *p < 0.05, **p < 0.01, ***p < 0.001).

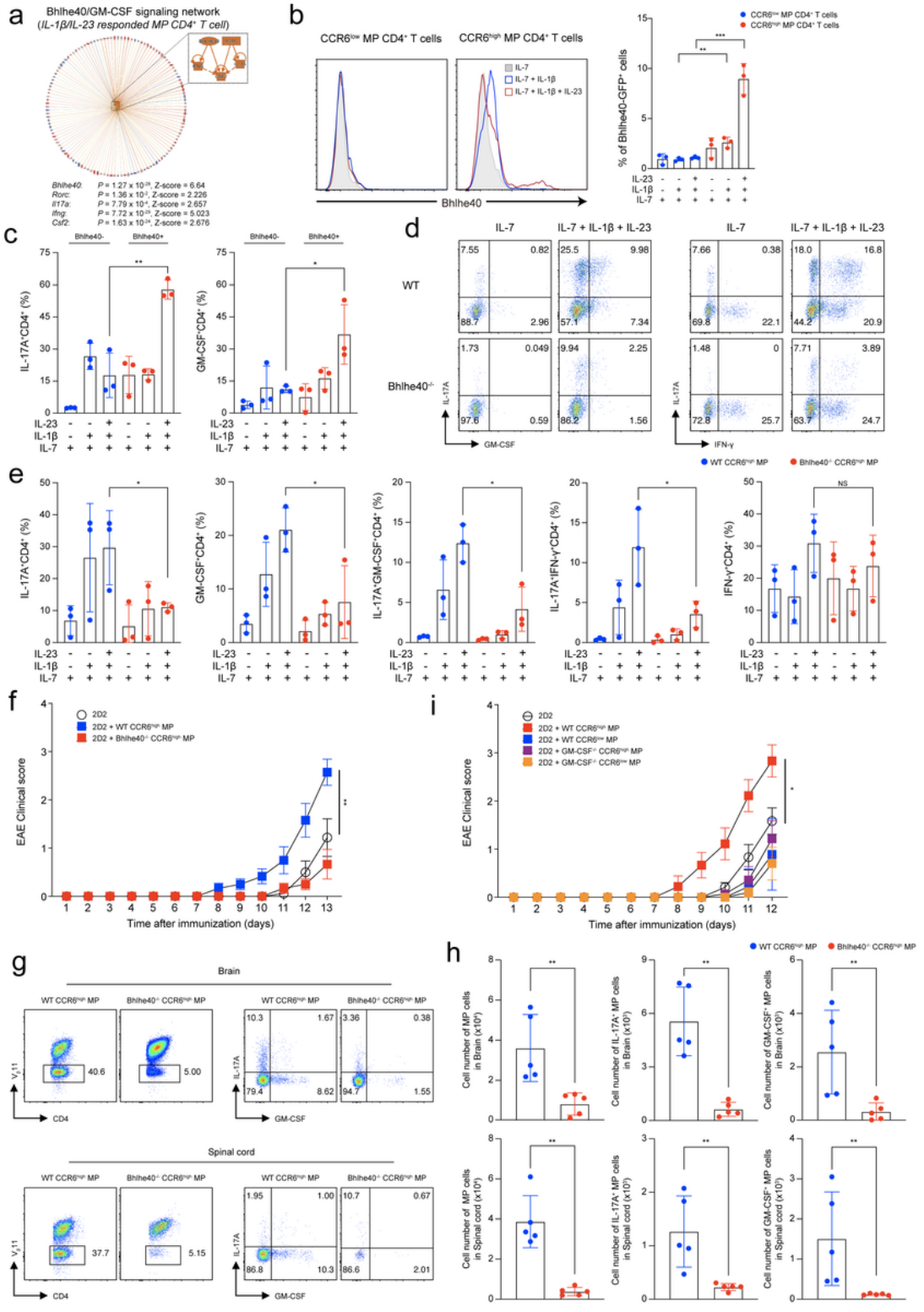

Figure 6

Innate-like effector functions of CCR6^{high} MP CD4^{+} T cells are conferred by Bhlhe40/GM-CSF axis.

(a) Predicted upstream network on IL-1β and IL-23 responded MP CD4^{+} T cells by IPA. (b) The representative histogram and average value showing the percentage of Bhlhe40 level in CCR6^{high} and CCR6^{low} MP CD4^{+} T cells induced by IL-1β/IL-23 stimulation without TCR engagement (n=3). (c) The representative percentage of IL-17A and GM-CSF expression compared to Bhlhe40^{GFP} positive and negative cells in CCR6^{high} MP CD4^{+} T cells induced by IL-1β /IL-23 without TCR engagement for 5 days (n=3). (d) Representative flow cytometry plots showing the cytokine expression and (e) average proportion of WT CCR6^{high} MP CD4^{+} T cells vs. Bhlhe40$^{-/-}$ CCR6^{high} MP CD4^{+} T cells (n = 3). (f) Naïve CD4^{+} T cells (5×10^{4}) from 2D2 transgenic mice were adoptively transferred, with or without WT CCR6^{high} or Bhlhe40$^{-/-}$ CCR6^{high} MP CD4^{+} T cells (1×10^{5}, CD45.1^{+}γδTCR^{-}NK1.1^{-}V$_{\beta}$11^{-}TCRβ^{+}CD4^{+}CD1d tetramer^{-} CD25^{-}CD62L^{low}CD44^{high}), into Rag$^{-/-}$ mice who were immunized with MOG$_{35-55}$ in CFA. EAE clinical score was monitored daily (n=5). (g) Representative flow cytometry plots and (h) absolute cell numbers of infiltrated 2D2 TCR (V$_{\beta}$11^{+})$^{-}$ MP CD4^{+} T cells (gating from CD45^{+}CD4^{+}) and IL-17A, GM-CSF, and IFN-γ producing cells from the spinal cords and brain on days 13 after immunization (n=5). (i) Naïve CD4^{+} T cells (5×10^{4}) from 2D2 transgenic mice were adoptively transferred, with or without WT CCR6^{high} or WT CCR6^{low} or GM-CSF$^{-/-}$ CCR6^{high} or GM-CSF$^{-/-}$ CCR6^{low} MP CD4^{+} T cells (1×10^{5}, CD45.1^{+}γδTCR^{-}NK1.1^{-} V$_{\beta}$11^{-}TCRβ^{+}CD4^{+}CD1d tetramer^{-}CD25^{-}CD62L^{low}CD44^{high}), into Rag$^{-/-}$ mice who were immunized with MOG$_{35-55}$ in CFA. EAE clinical score was monitored daily (n=9). Data are presented as the mean ± S.E.M in F and I and the mean ± S.D in b,c,d,e,g,h values were calculated using two-way ANOVA or Mann-Whitney U-test (NS, not significant; *p < 0.05, **p < 0.01, ***p < 0.001).

Supplementary Files

This is a list of supplementary files associated with this preprint. Click to download.

- Supplementaryinformation.docx